

3D NMR Experiments for Measuring ^{15}N Relaxation Data of Large Proteins: Application to the 44 kDa Ectodomain of SIV gp41

Michael Caffrey,* Joshua Kaufman,† Stephen J. Stahl,† Paul T. Wingfield,†
Angela M. Gronenborn,*¹ and G. Marius Clore*¹

*Laboratory of Chemical Physics, Building 5, National Institute of Diabetes and Digestive and Kidney Diseases, National Institutes of Health, Bethesda, Maryland 20892-0520; and †Protein Expression Laboratory, Building 6B, National Institute of Arthritis and Musculoskeletal and Skin Diseases, National Institutes of Health, Bethesda, Maryland 20892-2775

Received June 19, 1998; revised August 13, 1998

A suite of 3D NMR experiments for measuring ^{15}N - $\{^1\text{H}\}$ NOE, ^{15}N T_1 , and ^{15}N $T_{1\rho}$ values in large proteins, uniformly labeled with ^{15}N and ^{13}C , is presented. These experiments are designed for proteins that exhibit extensive spectral overlap in the 2D ^1H - ^{15}N HSQC spectrum. The pulse sequences are readily applicable to perdeuterated samples, which increases the spectral resolution and signal-to-noise ratio, thereby permitting the characterization of protein dynamics to be extended to larger protein systems. Application of the pulse sequences is demonstrated on a perdeuterated $^{13}\text{C}/^{15}\text{N}$ -labeled sample of the 44 kDa ectodomain of SIV gp41.

Key Words: ^{15}N relaxation; 3D NMR; large proteins; gp41.

Heteronuclear NMR spectroscopy has been extensively used to study protein dynamics (1). Typically, the ^{15}N - $\{^1\text{H}\}$ NOE, ^{15}N T_1 , and ^{15}N $T_{1\rho}$ or T_2 values are determined using a series of modified 2D ^1H - ^{15}N HSQC experiments (2–4). To characterize the dynamic properties of the individual N–H vectors, the experimental relaxation data are generally fit to the model-free formalism (5–7), although alternative methods have been proposed (cf. Ref. (4)). The dynamics of helical proteins with molecular weights greater than 20 kDa have proven difficult to characterize by NMR due to several factors: in particular, the reduction in signal-to-noise arising from increased $^1\text{H}_\text{N}$ transverse relaxation rates, and the increased spectral overlap arising from poor spectral dispersion characteristic of helical proteins. We have recently shown that modern multidimensional heteronuclear NMR experiments can be employed to obtain near-complete resonance assignments and determine the three-dimensional solution structure of the 44 kDa ectodomain of SIV gp41 (e-gp41, residues 27–149), a symmetric trimer comprising two long helices (residues 30–80 and 107–147) per subunit (8, 9). In the present communication, we present a suite of 3D NMR experiments designed to measure ^{15}N - $\{^1\text{H}\}$ NOE, ^{15}N T_1 , and ^{15}N $T_{1\rho}$ relaxation data in large proteins exhibiting extensive spectral overlap in the 2D ^1H - ^{15}N

HSQC spectrum, and demonstrate the applicability of these pulse sequences on perdeuterated $^{13}\text{C}/^{15}\text{N}$ -labeled SIV e-gp41.

The impetus for the design of 3D versions of the standard 2D ^{15}N relaxation experiments was the poor spectral dispersion of SIV e-gp41. Indeed only 50% of the ^1H - ^{15}N correlations are resolved in the 2D ^1H - ^{15}N HSQC spectrum of SIV e-gp41 (cf. Fig. 1A of Ref. (8)). Essentially all correlations, however, are resolved in the 3D HNCO experiment, which was previously exploited to determine H_N exchange rates (8). Thus, our strategy for designing 3D ^{15}N relaxation experiments is based on the incorporation of traditional 2D ^{15}N relaxation experiments (2–4) into the 3D constant time HNCO experiment (10). The resulting pulse sequences for determining ^{15}N - $\{^1\text{H}\}$ NOE, ^{15}N T_1 , and ^{15}N $T_{1\rho}$ are depicted in Figs. 1a, b, and c, respectively. Pulsed field gradients have been added to suppress undesired coherence pathways (11) and the WATERGATE sequence has been added for water suppression (12).

The experiments shown in Fig. 1 have been applied to perdeuterated $^{13}\text{C}/^{15}\text{N}$ -labeled SIV e-gp41. Figure 2a shows a $^{13}\text{CO}(F_1)$ - $^1\text{H}_\text{N}(F_3)$ plane from the 3D experiment designed to determine ^{15}N - $\{^1\text{H}\}$ NOE (pulse scheme in Fig. 1a), with the reference spectrum on the left and the NOE spectrum on the right. It can be seen that sufficient signal-to-noise and resolution is readily achieved for this large helical protein in a reasonable measurement time (43 h per experiment). It should also be noted that the correlations for Asp45 and Val119 are not resolved in the 2D ^1H - ^{15}N HSQC spectrum but are clearly separated by their ^{13}CO frequencies in the 3D experiment, thereby permitting the determination of their ^{15}N - $\{^1\text{H}\}$ NOE values. From the 3D experiment, the ^{15}N - $\{^1\text{H}\}$ NOE values for Asp45, Val119, and Ile126 are estimated to be 0.9 ± 0.1 , 0.8 ± 0.1 , and 0.9 ± 0.1 , respectively. Their magnitude indicates that these NH vectors do not exhibit large-amplitude internal motions, consistent with their location in the well-defined N- (residues 30–80) and C- (residues 107–147) terminal helices (9). ^{15}N T_1 decay

¹ To whom correspondence should be addressed.

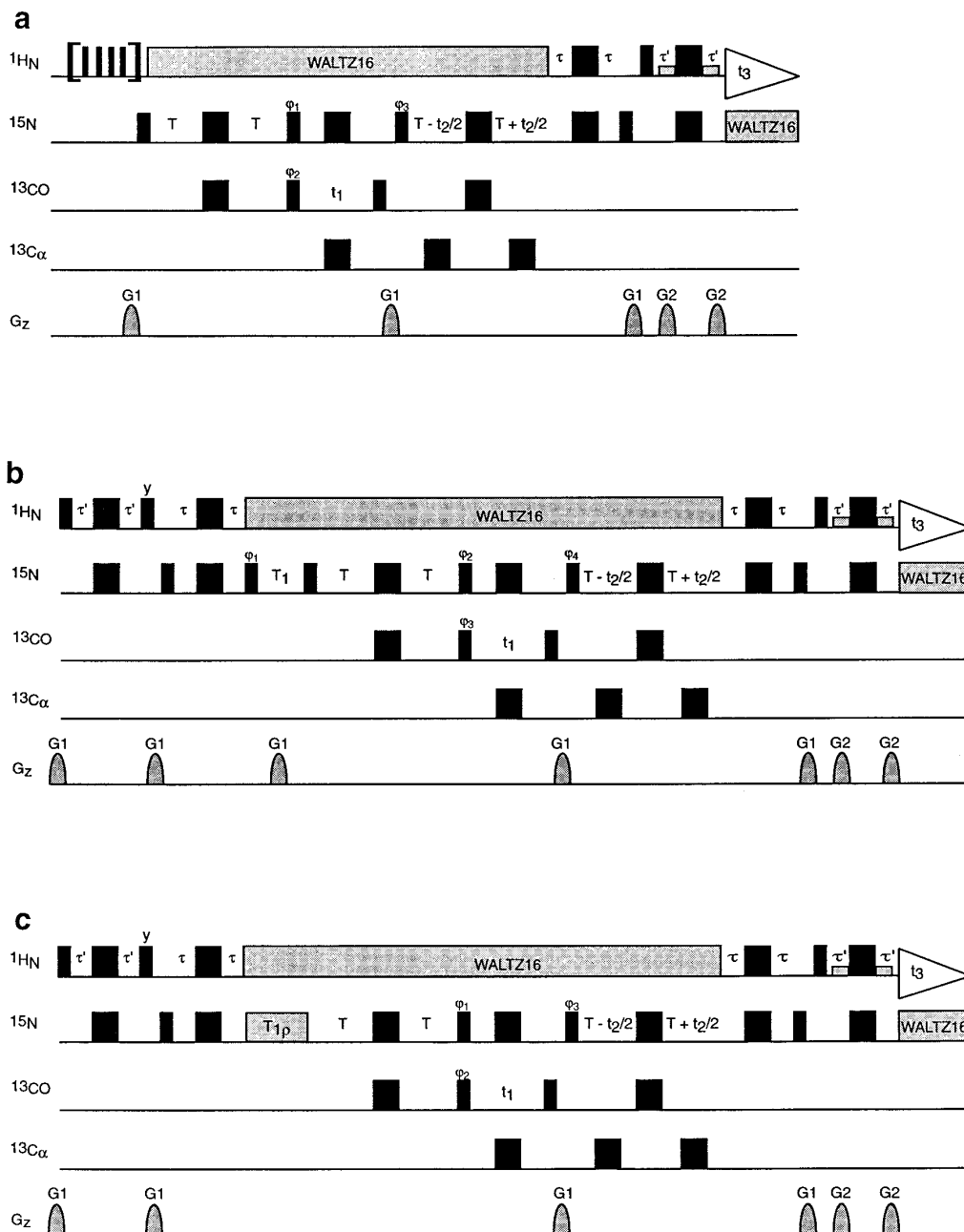


FIG. 1. 3D pulse sequences for the determination of (a) ^{15}N - $\{^1\text{H}\}$ NOE, (b) ^{15}N T_1 , and (c) ^{15}N $T_{1\rho}$. Thin and thick vertical bars represent 90° and 180° pulses, respectively. The delays τ' , τ , and T are set to 2.25, 2.7, and 13.5 ms, respectively. Quadrature detection in t_1 (^{13}CO) and t_2 (^{15}N) is achieved by incrementing φ_2 and φ_3 independently according to the States-TPPI method (16). Phase cycling in sequences (a) and (c) is as follows: $\varphi_1 = y, -y$; $\varphi_2 = 2(x), 2(-x)$; $\varphi_3 = 4(x), 4(-x)$; receiver = $x, 2(-x), x, -x, 2(x), -x$. Phase cycling in sequence (b) is $\varphi_1 = y, -y$; $\varphi_2 = 2(y), 2(-y)$; $\varphi_3 = 4(x), 4(-x)$; $\varphi_4 = 8(x), 8(-x)$; receiver = $x, 2(-x), x, -x, 2(x), -x, -x, 2(x), -x, x, 2(-x), x$. WALTZ-16 (17) is used for ^1H and ^{15}N decoupling. In sequence (a), ^1H saturation is accomplished by a series of 120° pulses during the relaxation delay. In sequence (c), the boxed $T_{1\rho}$ delay represents a 1–3 kHz ^{15}N spin lock. The gradients are sine bell-shaped, 25 G/cm at the center, and applied for the following durations: $G_1 = 3$ ms, $G_2 = 0.6$ ms. Experiments (b) and (c) are carried out for several different values of the delays T_1 and $T_{1\rho}$, respectively. For optimal sensitivity the relaxation delay should be set to $\sim 1.3 \times ^1\text{H}_\text{N} T_1$ in (b) and (c) (18). Note that a water flip back pulse along $-x$ (applied as either a half-Gauss-shaped 90° pulse or a soft rectangular 90° pulse of duration ~ 2.5 ms) between the hard ^{15}N and ^1H 90° pulses of the last INEPT sequence is readily introduced in pulse scheme (a) to avoid saturation of the water resonance (19).

curves obtained using the pulse scheme in Fig. 1b are shown in Fig. 2b for Ser29, Val58, Phe88, Ala128, and Asn140, and yield ^{15}N T_1 values of 710 ± 8 , 974 ± 133 , 651 ± 23 ,

902 ± 28 , and 922 ± 75 ms, respectively. The corresponding ^{15}N $T_{1\rho}$ decay curves obtained using the pulse scheme in Fig. 1c are shown in Fig. 2c and yield ^{15}N $T_{1\rho}$ values of

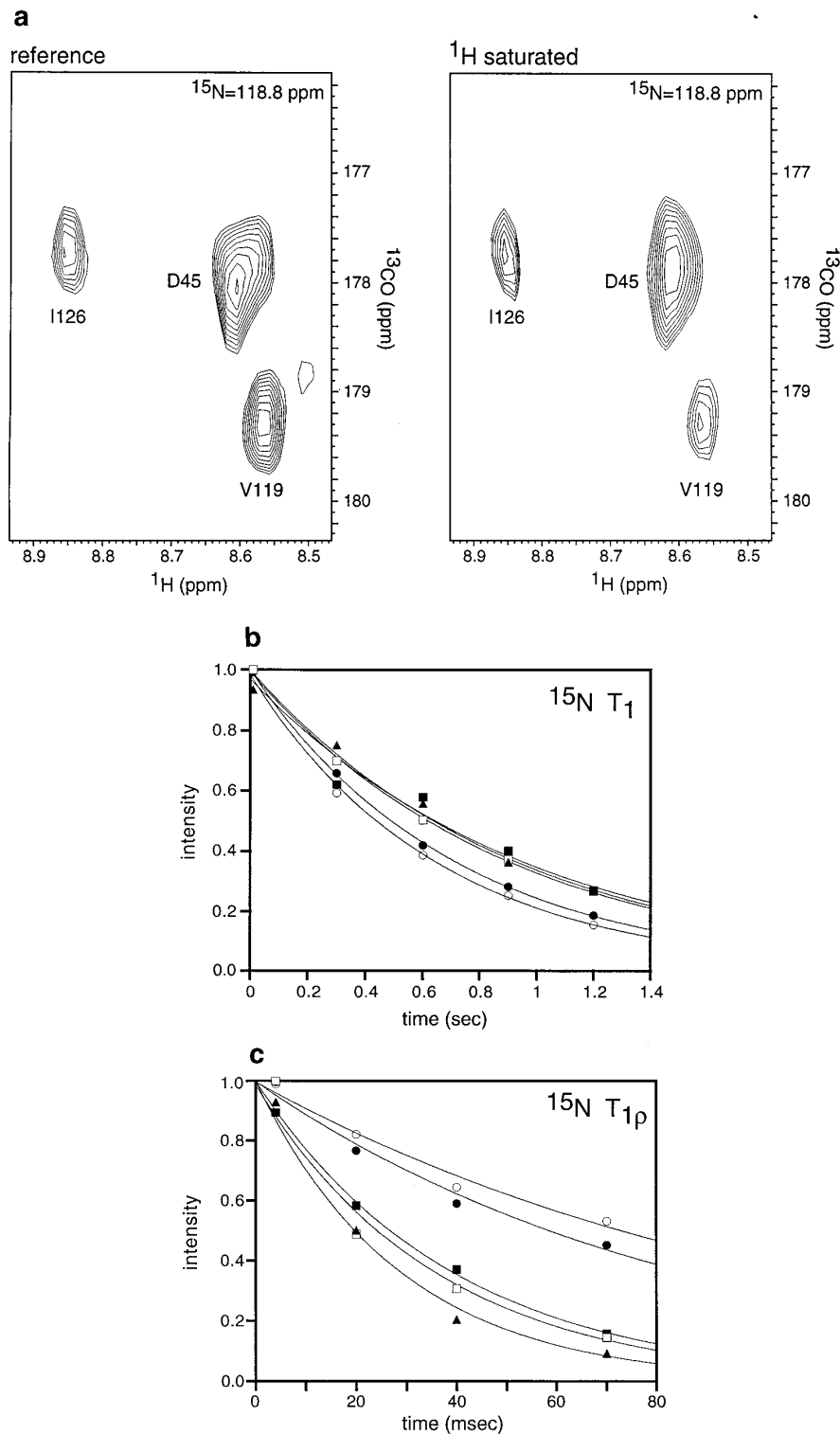


FIG. 2. (a) $^{13}\text{CO}(F_1)$ - $^1\text{H}(F_3)$ plane of the 3D reference and ^1H saturated spectra used to measure ^{15}N - $\{^1\text{H}\}$ NOE. (b) Decay curves obtained using the pulse schemes in Figs. 1b and c to determine (b) the $^{15}\text{N } T_1$ and (c) $^{15}\text{N } T_{1\rho}$ relaxation times of Ser29 (●), Val58 (■), Phe88 (○), Ala128 (□), and Asn140 (▲). All spectra were recorded on a Bruker DMX500 spectrometer. Sample conditions were 2 mM uniformly $^2\text{H}/^{13}\text{C}/^{15}\text{N}$ -labeled e-gp41 (monomer concentration) in 50 mM sodium formate, pH 3.0, and 90% $\text{H}_2\text{O}/10\%$ D_2O at 45°C. ^{15}N and ^{13}C labeling was $>95\%$, and ^2H labeling $\geq 80\%$. Spectral widths for ^1H , ^{13}C , and ^{15}N were 16, 10, and 26 ppm, respectively, with the carrier positions set to 4.58, 178, and 120 ppm, respectively. ^{13}CO and $^{13}\text{C}\alpha$ pulses were applied at 178 and 56 ppm, respectively. The $^{13}\text{C } 90^\circ$ and 180° pulse lengths were set to 63.1 ($15^{1/2}/4\Delta$) and 56.6 ($3^{1/2}/2\Delta$) μs , respectively (where Δ is the frequency difference in Hz between the carrier positions for the ^{13}CO and $^{13}\text{C}\alpha$ pulses), such that when applied at the ^{13}CO frequency the pulses have a null

84.7 ± 8.2 , 38.5 ± 1.3 , 106 ± 10.6 , 35.6 ± 4.1 , and 28.4 ± 1.3 ms, respectively. Each time point for the ^{15}N T_1 and $T_{1\rho}$ experiments was acquired in approximately 4.5 h. Ser29 and Phe88 are located in relatively mobile regions (9), consistent with their relatively shorter ^{15}N T_1 and longer ^{15}N $T_{1\rho}$ values. Val58, Ala128, and Asn140, on the other hand, are located in helices (9), consistent with their relatively longer ^{15}N T_1 and shorter ^{15}N $T_{1\rho}$ values. The ^{15}N $T_1/T_{1\rho}$ ratios for the helical regions ranges from 25 to 32 at $\omega_{\text{H}} = 2\pi \times 500$ MHz, corresponding to an apparent correlation time of 18–22 ns. e-gp41 is a rod-shaped axially symmetric molecule, ~ 110 Å in length and ~ 34 Å in width. The inertia tensor calculated from the coordinates has an anisotropy of ~ 6.8 which corresponds to a predicted diffusion anisotropy of $6.8^{2/3} \sim 3.6$ (13). Since the helices, and hence the N–H vectors, are oriented at angles of 10° – 20° to the long axis of the molecule (9), the apparent correlation time of 18–22 ns corresponds approximately to the correlation time along the z axis of the diffusion tensor (i.e., $\sim D_{zz}^{-1}$). Assuming a diffusion anisotropy of ~ 3.6 , the predicted effective correlation time, given by $(2D_{zz} + 2D_{yy} + 2D_{xx})^{-1}$, is ~ 12 ns with minimum and maximum ^{15}N $T_1/T_{1\rho}$ ratios of ~ 9 and ~ 34 at $\omega_{\text{H}} = 2\pi \times 500$ MHz.

In conclusion, we have demonstrated that useful dynamic information can be derived from 3D versions of ^{15}N relaxation experiments performed on a 44 kDa protein. Sufficient signal-to-noise ratios are achieved due to the high sensitivity of the HNC0 experiment that forms the basic unit of the sequences. The requirement for uniform ^{13}C labeling can be expected to increase the relaxation rates by $\leq 5\%$ (15), which is small given the experimental errors. The present sequences are amenable to perdeuterated samples, which increases both spectral resolution and signal-to-noise. Previously, perdeuteration has been shown to have no measurable effect on ^{15}N relaxation parameters, although some of the increases in signal-to-noise are offset by the increased $^1\text{H}_\text{N}$ T_1 of perdeuterated samples (13). We expect that the present set of 3D ^{15}N relaxation experiments will prove useful for the characterization of the dynamic properties of large helical proteins. Moreover, these experiments should prove useful for dynamic studies of partially folded and unfolded proteins due to the increased resolution afforded by the ^{13}C chemical shift (cf. Ref. (14)). Finally, we note that 3D accordion spectroscopy has recently been proposed as an alternative method to measure ^{15}N (and ^{13}C) T_1 relaxation rates (15) for proteins that exhibit spectral overlap in the 2D relaxation experiments.

ACKNOWLEDGMENT

This work was supported by the AIDS Targeted Antiviral Program of the Office of the Director of the National Institutes of Health (to G.M.C., A.M.G., and the Protein Expression Laboratory).

REFERENCES

1. J. W. Peng and G. Wagner, Investigation of protein motions via relaxation measurements, *Methods Enzymol.* **239**, 563–596 (1994).
2. L. E. Kay, D. A. Torchia, and A. Bax, Backbone dynamics of proteins studied by ^{15}N inverse-detected heteronuclear NMR spectroscopy: Application to staphylococcal nuclease, *Biochemistry* **28**, 8972–8979 (1989).
3. G. M. Clore, P. C. Driscoll, P. T. Wingfield, and A. M. Gronenborn, Analysis of the backbone dynamics of interleukin-1 β using two-dimensional inverse detected heteronuclear ^{15}N - ^1H NMR spectroscopy, *Biochemistry* **29**, 7387–7401 (1990).
4. J. W. Peng and G. Wagner, Mapping spectral density functions using heteronuclear NMR relaxation measurements, *J. Magn. Reson.* **98**, 308–332 (1992).
5. G. Lipari and A. Szabo, Model-free approach to the interpretation of nuclear magnetic resonance relaxation in macromolecules. 1. Theory and range of validity, *J. Am. Chem. Soc.* **104**, 4546–4559 (1982).
6. G. Lipari and A. Szabo, Model-free approach to the interpretation of nuclear magnetic resonance relaxation in macromolecules. 2. Analysis of experimental results, *J. Am. Chem. Soc.* **104**, 4546–4559 (1982).
7. G. M. Clore, A. Szabo, A. Bax, L. E. Kay, P. C. Driscoll, and A. M. Gronenborn, Deviations from the simple two-parameter model-free approach to the interpretation of nitrogen-15 nuclear magnetic relaxation of proteins, *J. Am. Chem. Soc.* **112**, 4989–4991 (1990).
8. M. Caffrey, M. Cai, J. Kaufman, S. J. Stahl, P. T. Wingfield, A. M. Gronenborn, and G. M. Clore, Determination of the secondary structure and global topology of the 44 kDa ectodomain of gp41 of Simian immunodeficiency virus by multidimensional nuclear magnetic resonance spectroscopy, *J. Mol. Biol.* **271**, 819–826 (1997).
9. M. Caffrey, M. Cai, J. Kaufman, S. J. Stahl, P. T. Wingfield, D. G. Covell, A. M. Gronenborn, and G. M. Clore, Three-dimensional solution structure of the 44 kDa ectodomain of SIV gp41, *EMBO J.* **17**, 4572–4584 (1998).
10. S. Grzesiek and A. Bax, Improved 3D triple-resonance NMR techniques applied to a 31 kDa protein, *J. Magn. Reson.* **96**, 432–440 (1992).
11. A. Bax and S. Pochapsky, Optimized recording of heteronuclear multidimensional NMR spectra using pulsed field gradients, *J. Magn. Reson.* **99**, 638–643 (1992).
12. M. Piotto, V. Saudek, and V. Sklenar, Gradient-tailored excitation for single quantum NMR spectroscopy of aqueous solutions, *J. Biomol. NMR* **2**, 661–665 (1992).
13. N. Tjandra, P. T. Wingfield, S. J. Stahl, and A. Bax, Anisotropic rotational diffusion of perdeuterated HIV protease from ^{15}N NMR

excitation at the $^{13}\text{C}\alpha$ frequency, and vice versa. Spectra were acquired with 10 complex points in t_1 and 20 complex points in t_2 . The spectra in (a) correspond to 64 scans per increment and a relaxation/saturation time of 3 s, resulting in an experimental time of ~ 43 h for each spectrum. The spectra in (b) and (c) were recorded with 16 scans per increment and a relaxation delay of 1.2 s, resulting in experimental times of ~ 4.5 h per time point. The time points were 50, 300, 600, 900, and 1200 ms for (b), and 4, 20, 40, and 70 ms for (c), and the continuous lines represent single exponential least-squares best fits to the experimental data. Spectra were processed using the program NMRPipe (20).

- relaxation measurements at two magnetic fields, *J. Biomol. NMR* **8**, 273–284 (1996).
14. J. Yao, J. Dyson, and P. E. Wright, Chemical shift dispersion and secondary structure prediction in unfolded and partially folded proteins, *FEBS Lett.* **419**, 285–289 (1997).
 15. P. A. Carr, D. A. Fearing, and A. G. Palmer, 3D accordion spectroscopy for measuring ^{15}N and ^{13}CO relaxation rates in poorly resolved NMR spectra, *J. Magn. Reson.* **132**, 25–33 (1998).
 16. D. Marion, M. Ikura, R. Tschudin, and A. Bax, Rapid recording of 2D NMR spectra without phase cycling. Application to the study of hydrogen exchange in proteins, *J. Magn. Reson.* **85**, 393–399 (1989).
 17. A. J. Shaka, J. Keeler, T. Frenkiel, and R. Freeman, An improved sequence for broadband decoupling: WALTZ-16, *J. Magn. Reson.* **52**, 335–338 (1983).
 18. J. Cavanagh, W. J. Fairbrother, A. G. Palmer III, and N. J. Skelton, "Protein NMR Spectroscopy: Principles and Practice," Academic Press, New York (1996).
 19. S. Grzesiek and A. Bax, The importance of not saturating H_2O in protein NMR: Application to sensitivity enhancement and NOE measurements, *J. Am. Chem. Soc.* **115**, 12593–12594 (1993).
 20. F. Delaglio, S. Grzesiek, G. W. Vuister, G. Zhu, J. Pfeifer, and A. Bax, NMRPipe: A multidimensional spectral processing system based on UNIX pipes, *J. Biomol. NMR* **6**, 277–293 (1995).